# Crystal morphology prediction and experimental verification of venlafaxine hydrochloride

Chenjing Liang,[1] Jianghai Zhuang,[2] Chenghan Zhuang,[2] Zhaoxia Zhang,[1] Guanglie Lv,[3] and Guoqing Zhang[1,a)]
[1]School of Materials Science and Engineering, Zhejiang Sci-Tech University, Hangzhou 310018, China
[2]Zhejiang Apeloa Jiayuan Pharmaceutical Co., Ltd., Dongyang 322118, China
[3]Zhejiang University, Hangzhou 310018, China

(Received 5 May 2022; accepted 1 August 2022)

This paper aims to explore the influence of solvent effects on the crystal habit of venlafaxine hydrochloride using the modified attachment energy (MAE) model by molecular dynamics (MD) simulation. Solvent effects were investigated based on the different morphologies of venlafaxine hydrochloride acquired by simulation and experimental technology from the solvents of isopropanol, dimethyl sulfoxide, and acetonitrile. Firstly, morphologically dominant crystal faces were obtained through the prediction of crystal habit in vacuum by the attachment energy (AE) model. Subsequently, the MAEs were calculated by the MD simulation to modify the crystal shapes in a real solvent environment, and the simulation results were in agreement with the experimental ones. Meanwhile, in order to have a better understanding of the solvent effects, the surface structure was introduced to analyze the solvent adsorption behaviors. The results show that the crystal habits of venlafaxine hydrochloride are affected by the combination of the AE and surface structures. Finally, the flowability of the obtained crystal powders from different solvents was investigated by measurement and analysis of the angle of repose and compressibility. The above results verify that the physical properties are closely related to the morphologies of the crystals.  [doi:10.1017/S0885715622000264]

Key words: crystal habit, solvent effect, molecular dynamics simulation, surface structure, intermolecular interaction

## I. INTRODUCTION

The crystal morphology of a drug plays a crucial role in pharmaceutical manufacturing, having a strong influence on its chemical and physical properties such as filtration, compaction behavior, and powder flow properties (MacLeod and Muller, 2012; Jiang *et al.*, 2013). In practice, recrystallization in different solvents is one of the main ways to prepare drug crystals with various morphologies (Miroslav *et al.*, 2012). Therefore, it has been indispensable to explore the crystal growth and habits under different solvents in industrial production. As indicated by many researchers (Liu *et al.*, 2007; Salvalaglio *et al.*, 2012; Urbelis and Swift, 2014), the interactions between solvent molecules and crystal faces are essential to crystal growth. Hence, in order to obtain desired crystal shapes, it is necessary to investigate solvent effects on crystal habits.

Although drug crystals with various morphologies can be prepared through crystallization experiments, it takes a lot of time and manpower to find the optimal one that benefits production. In recent years, some computer-aided methods have been explored to predict or design the growth of crystals, among which the most representative ones are molecular simulation and first principles simulation (Khoshkhoo and Anwar, 1996; Graaf *et al.*, 2012; Zhang *et al.*, 2013; Dzade *et al.*, 2016). Compared to the crystallization experiment based on "trial and error method", predicting the crystal shape by a theoretical method is helpful to deeply understand the crystal growth mechanism from the microscopic point of view, and can quickly screen the crystallization conditions such as solvent and temperature, thus providing a broader perspective for crystal morphology research and industrial production.

Molecular dynamics (MD) is one of the simulation methods that analyses crystal growth direction at the molecular level based on the molecular structure, revealing the interaction between solvent molecules and crystal surfaces. The crystal morphologies of more and more substances have been successfully predicted with the maturity of this technology, providing detailed guidance for laboratory and industrial crystallization. Zhu *et al.* (2020) utilized a modified attachment energy model (MAE) to simulate the crystal habits of catechol obtained from three different solvents of isopropanol, methyl acetate, and ethyl acetate and disclosed the reason for different crystal morphology forming from the molecular point of view. Li *et al.* (2019) adjusted the growth rate of $\beta$-HMX surfaces by changing the ratio of water/ethanol, revealing that the water/ethanol ratio, temperature, and supersaturation would affect the crystal morphology of $\beta$-HMX. Zhang *et al.* (2017)

a)Author to whom correspondence should be addressed. Electronic mail: zgq@zstu.edu.cn

 

simulated the crystal morphology of ibuprofen obtained from four different solvents using the MAE model and found that solvents have a great influence on the aspect ratio of crystals, suggesting that this method has a great prospect in the field of rapid solvent screening.

Venlafaxine hydrochloride is a derivative of phenylethylamine, which is mainly used to treat various kinds of depression and generalized anxiety disorder (Andrews *et al.*, 1996). Compared with other antidepressants, venlafaxine hydrochloride has obvious advantages such as high cure rate, quick curative effect, and less drug interaction (Lecrubier *et al.*, 1997; Olver *et al.*, 2001). The current research emphasis is usually focused on its synthesis techniques and crystal form development (Xu and Wang, 2017). Further experimental and simulation investigations on venlafaxine hydrochloride crystal morphology and microstructure are necessary to get a deeper insight into the crystal growth and habits, which helps to select optimal crystal shapes and improve product quality for industrial production.

In this paper, the morphologies of venlafaxine hydrochloride recrystallized from isopropanol, dimethyl sulfoxide, and acetonitrile were simulated using the MAE model. Meanwhile, recrystallization experiments in several solvents were conducted to prepare the crystals with different morphologies for model verification. The solvent effects on crystal habits from the perspective of crystal–solvent interactions and surface structure were described, which may favor a better understanding of crystal growth from the microscopic point of view.

## II. CALCULATION METHODOLOGY

### A. Theory

At present, the models used to predict crystal habits include Bravais–Friedel–Donnay–Harker (BFDH) criterion, attachment energy (AE) model, occupancy model, interface structure analysis model, screw dislocation growth model, 2D nucleation model, and Ising model (Liu, 2021). The principles of these methods evolved from structural and energy factors to growth mechanism. Among them, the AE model has become the most widely used in crystal shape prediction based on the consideration of crystal structure and energy factors (Hartman and Bennema, 1980). AE ($E_{att}$) is defined as the released energy when a growth slice attaches to a growing crystal surface. The relative growth rate ($R_{hkl}$) of each crystal face (*h k l*) is assumed to be proportional to the absolute value of the AE:

$$R_{hkl} \propto |E_{att}| \tag{1}$$

The AE ($E_{att}$) is calculated as

$$E_{att} = E_{latt} - E_{slice} \tag{2}$$

where $E_{latt}$ stands for the lattice energy, $E_{slice}$ represents the energy of a growth slice with a thickness of $d_{hkl}$.

The AE model is most suitable for simulation of crystal morphology in vacuum environment, but in practice, a large number of crystals grow from solvents, where solvent molecules will adsorb on the crystal surfaces as solute molecules do, which means the growth of the crystal faces may be blocked because of the adsorption of the solvent molecule (Weissbuch *et al.*, 1991). To predict the impact of a solvent on the crystal morphology, an energy correction term, $E_S$, for the vacuum AE, $E_{att}$, is introduced to represent this solvent effect. The MAE, $E'_{att}$, can be calculated as follows:

$$E'_{att} = E_{att} - E_s \tag{3}$$

where $E_s$ represents the binding energy between the solvent molecules and the crystal face, which can be obtained using the following equation:

$$E_s = E_{int} \times \frac{A_{acc}}{A_{box}} \tag{4}$$

where $A_{box}$ is the total crystal surface area of the simulated supercell along the (*h k l*) direction, and $A_{acc}$ represents the solvent-accessible area of the crystal face in the unit cell. $E_{int}$ is defined as the interaction energy between a specific crystal face and the corresponding solvent layer, which can be calculated as follows:

$$E_{int} = E_{tot} - (E_{sur} + E_{sol}) \tag{5}$$

where $E_{tot}$ means the total energy of the entire simulation box including all crystal and solvent molecules, and $E_{sur}$ and $E_{sol}$ represent the energy of the isolated crystal surface and solvent layer, respectively. After correction, the relative growth rate $R'_{hkl}$ in the MAE model was still in proportion to the absolute value of the MAE $|E'_{att}|$:

$$R'_{hkl} \propto |E'_{att}| \tag{6}$$

### B. Simulation details

The crystal structure data of venlafaxine hydrochloride (form II) was obtained from Acta Crystallographica Section E, derived from experiments by A. Sivalakshmidevi *et al.* (2002) with the space group of $P2_1/n$ ($a = 5.797$ Å, $b = 26.074$ Å, $c = 11.722$ Å, $\alpha = \gamma = 90°$, $\beta = 100.72°$). The molecular structure and the crystal packing figure of venlafaxine hydrochloride are shown in Figure 1,

All the geometry optimization and MD simulations were performed with the Forcite module of Materials Studio 8.0 under the COMPASS force field. As the first molecular force field based on *ab initio* calculation, it can accurately predict the molecular structure, conformation, vibration, and thermodynamic properties of isolated and condensed molecules. As shown in Table I, the lattice parameters of the experimental crystal are in good agreement with the optimized via the COMPASS force field with the relative error of each parameter less than 3.02%, which indicates the implementation of MD simulations on venlafaxine hydrochloride is reasonable and feasible by the COMPASS force field (Figure 2).

After geometry optimization, the morphology of venlafaxine hydrochloride was predicted in vacuum through the Morphology module, and a list of possible growing crystal faces existing in the solution environment was obtained. Subsequently, these dominant faces are cleaved separately from the crystal and extended to a 3D periodic supercell. At present, there is no general rule for the construction of supercells, but taking the balance between accuracy and time into consideration, most researchers select a $3 \times 3 \times 3$ crystal face



https://doi.org/10.1017/S0885715622000264 Published online by Cambridge University Press

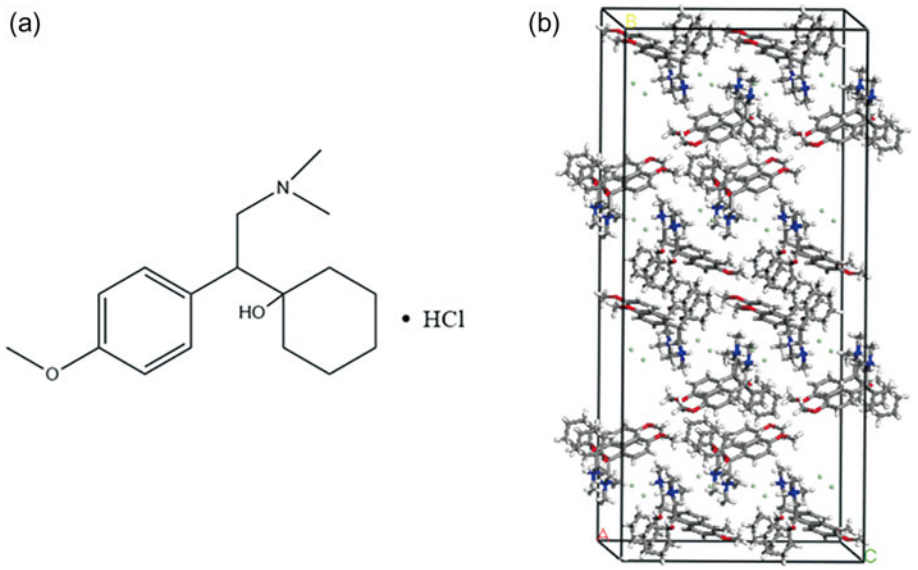


Figure 1. The molecular structure (a) and the crystal packing figure (b) of venlafaxine hydrochloride.

model when building supercells. To improve the accuracy of simulation results, the three-dimensional periodic solvent box containing 300 randomly distributed solvent molecules was constructed by the Amorphous Cell tool, and the size of the solvent box was consistent with the length and width of the crystal supercell.

Further, a double-layer crystal–solvent interface model was constructed and a vacuum box with a thickness of 50 Å was set up above the solvent layer to eliminate influence of other free boundaries. After further geometric optimization of the double-layer structure model, the MD simulation was carried out with an NVT ensemble at 298 K, with a total duration of 200 ps at a time step of 1 fs. The data were collected every 5000 steps to search the equilibrium state with the lowest energy of the whole system under the Andersen thermostat. In terms of energy setting, the standard Ewald method was used to calculate the electrostatic interactions with an accuracy of 0.0001 kcal $mol^{-1}$, meanwhile, the atom-based summation method was applied to calculate van der Waals interactions with a cutoff distance (dc) of 15.5 Å.

## III. EXPERIMENT AND CHARACTERIZATION

### A. Materials

Commercial venlafaxine hydrochloride (99.99% purity) was supplied by Apeloa Jiayuan Pharmaceutical Co., Ltd. (Dongyang, China). Isopropanol, dimethyl sulfoxide, and acetonitrile were provided by Hangzhou Mick Chemical Instrument Co., Ltd. (Hangzhou, China). All reagents were analytical grade and used without further purification.

TABLE I. The comparison of the initial and the optimized lattice parameters of venlafaxine hydrochloride.

| Lattice parameter | $a$ (Å) | $b$ (Å) | $c$ (Å) | $\alpha$ (°) | $\beta$ (°) | $\gamma$ (°) |
|---|---|---|---|---|---|---|
| Experiment | 5.797 | 26.074 | 11.722 | 90 | 100.720 | 90 |
| COMPASS optimized | 5.957 | 26.064 | 11.933 | 90 | 103.766 | 90 |
| Relative error (%) | 2.760 | 0.038 | 1.800 | 0 | 3.020 | 0 |

### B. Cooling crystallization experiments

Crystals of venlafaxine hydrochloride were obtained by natural cooling recrystallization in isopropanol, dimethyl sulfoxide, and acetonitrile, respectively. In a typical experiment, excess venlafaxine hydrochloride was added to a certain amount of solvent at room temperature and then heated to 70 °C for 2 h until it was dissolved totally. The solution naturally cools to room temperature, resulting in the precipitation of venlafaxine hydrochloride crystals. Finally, crystal powders with different morphologies were obtained by filtation and drying at 40 °C.

### C. Crystal characterization

The crystal forms of the crystal products were characterized by a powder X-ray diffractometer (XRD, Bruker D8 Advance) at a scanning rate of 2°/min. The XRD data were collected using Cu$K\alpha$ radiation and the $2\theta$ scan range was 3°–40°. Then samples were observed on a field emission scanning electron microscope (FSEM, Zeiss GeminiSEM500). The fluidity of these samples was characterized by a particle and powder characteristic analyzer (Rooko FT-2000A).

## IV. RESULTS AND DISCUSSION

### A. XRD characterization and analysis of the crystalline products

Generally, the crystal morphology of drugs is likely to change because of polymorphism. Furthermore, a polymorph form can also exhibit different morphology because of crystal habit. Many researches indicate that there is a significant difference in crystal morphology for the crystal products obtained from different solvents (Kitamura and Ishizu, 2000; Ter Horst *et al.*, 2002; Parmar *et al.*, 2007). The difference will lead to various physical and chemical properties such as particle size, flowability, apparent solubility, and thermostability. Therefore, it is necessary to examine the crystal growth in different solvents.



https://doi.org/10.1017/S0885715622000264 Published online by Cambridge University Press

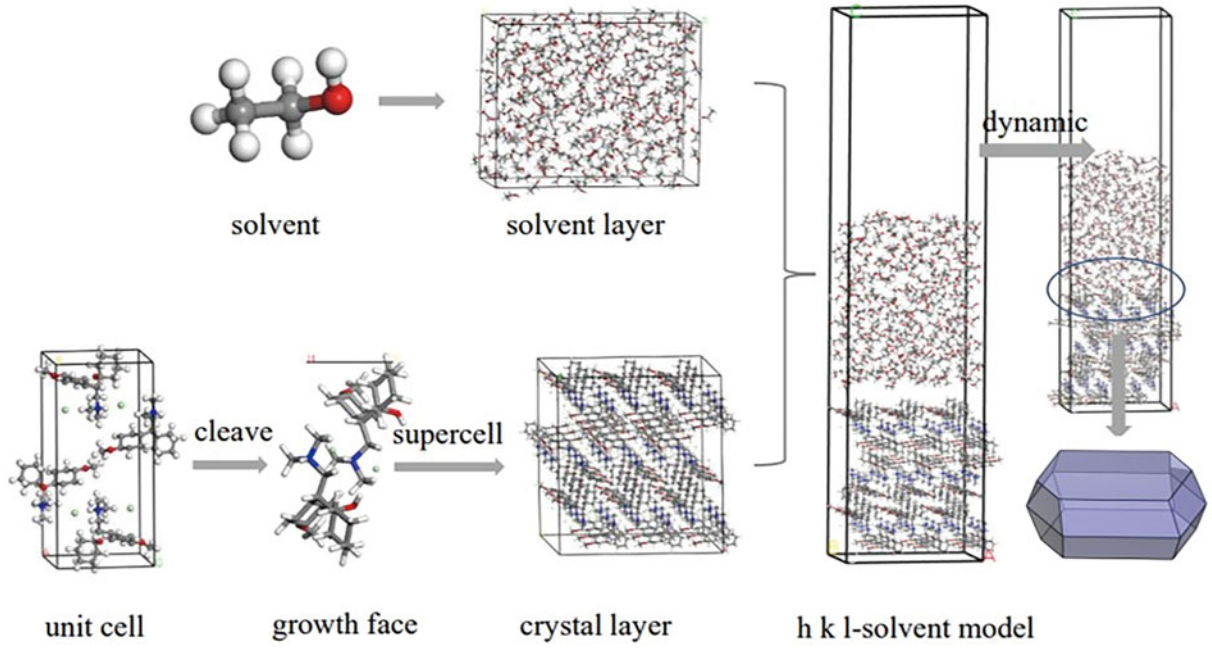


Figure 2. Diagram of simulation process (Chen *et al.*, 2020).

As illustrated in Figure 3, the venlafaxine hydrochloride products crystallized from isopropanol, dimethyl sulfoxide, and acetonitrile have similar characteristic peaks consistent with the raw material, proving that all the samples were in the same crystal form as reported.

To analyze the patterns in depth, one can see there are marked differences in the intensities of the diffraction peaks compared with the diffraction pattern derived from single crystal data, meaning preferred orientation growth occurs in some crystal faces, such as (0 0 1), (1 0 1), and (1 0 0) at 6.79°, 8.40°, and 10.26°, respectively. These changes reflect the forming of the crystal habits during the crystal growth in various solvents.

To further illustrate the preferred orientation of venlafaxine hydrochloride crystal theoretically, the corresponding polar figures based on their X-ray diffraction data are introduced, and the polar figures of (0 2 0) and (0 1 1) faces as examples are selected and shown in Figure 4. It is clear that the texture intensity of the (0 2 0) face is stronger than that of the (0 1 1) face, no matter which solvent the crystal is cultured in. Especially from Figure 4(b), the (0 1 1) face polar figure shows extremely uniform density distribution, indicating the crystal has no remarkable orientation on the (0 1 1) face.

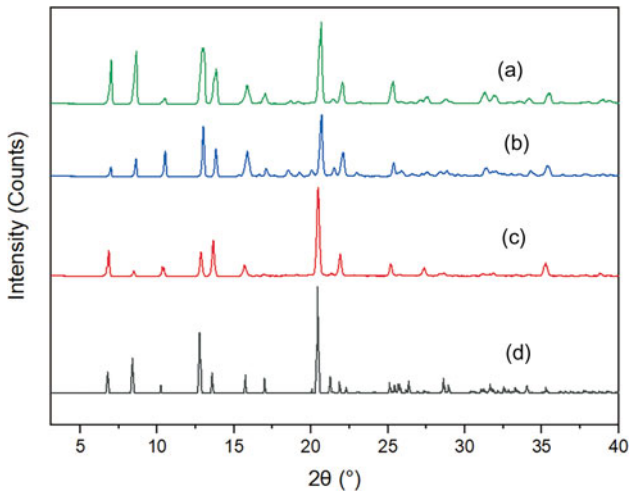


Figure 3. Powder X-ray diffraction (PXRD) patterns of the venlafaxine hydrochloride crystals crystallized from (a) isopropanol, (b) acetonitrile, (c) dimethyl sulfoxide, and (d) calculated from single crystal data.

### B. Prediction of venlafaxine hydrochloride crystal morphology in vacuum

In order to understand the crystal growth process, a series of simulations were performed. The vacuum morphology of venlafaxine hydrochloride with seven dominant surfaces calculated by the AE model is constructed and exhibited in Figure 5(a). The platelike crystal with seven dominant faces reflects not only crystallography geometry, but also intermolecular interactions at a deeper level. Figure 5(b) visualizes the interactions between the venlafaxine hydrochloride molecules generated by the Crystal Graph in the morphology module, where the blue, red, gray, and green lines, respectively, represent the interaction from strong to weak. Numerous studies have suggested that crystals grow faster along the direction with strong molecular interactions (Zhao *et al.*, 2016). Therefore, venlafaxine hydrochloride crystals grow faster along the direction of the blue and red lines than the gray and green lines. Based on the periodic bond chain (PBC) theory, the fastest-growing direction is the strongest bond direction. The surfaces with a fast growth rate may disappear, while the surfaces with a slow growth rate will appear in the final morphology, which plays a decisive role in the final shape of the crystal.

On the basis of Crystal Graph, Hirshfeld surface analysis was used to investigate intermolecular interactions in the venlafaxine hydrochloride crystal. As shown in Figure 6, where $d_i$ and $d_e$ denote the distance from the surface to the nearest atom



https://doi.org/10.1017/S0885715622000264 Published online by Cambridge University Press

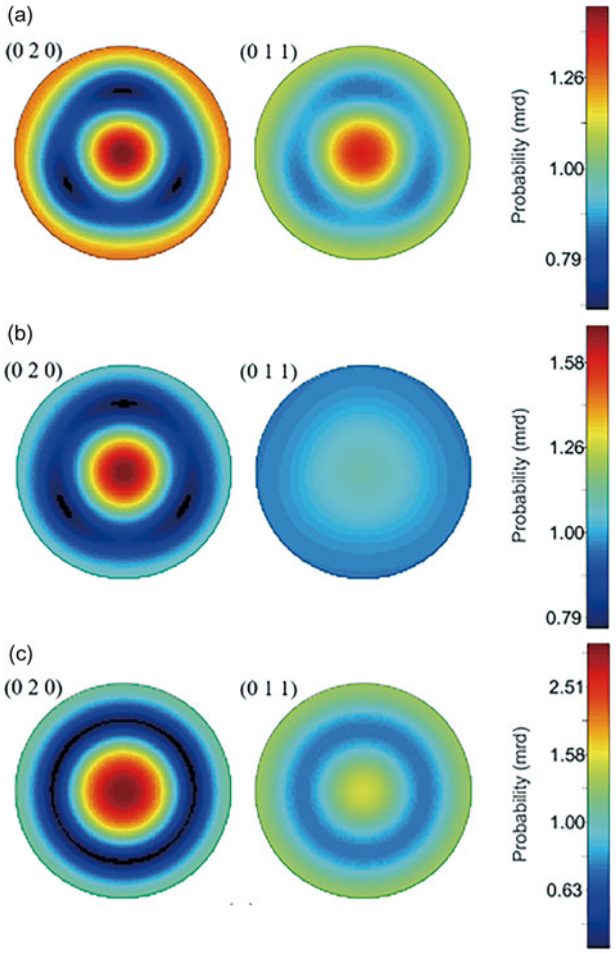


Figure 4. Polar figures of (0 2 0) and (0 1 1) faces of the venlafaxine hydrochloride crystals crystallized from (a) isopropanol, (b) dimethyl sulfoxide, and (c) acetonitrile.

interior or exterior to the surface respectively, while $d_{norm}$ is a normalized contact distance (Spackman and Mckinnon, 2002; Mckinnon *et al.*, 2007; Spackman and Jayatilaka, 2009). The figure separately depicts the individual hydrogen bonding interactions on the $d_{norm}$ surfaces. Also, the strong hydrogen bonding contacts are depicted as large circular depressions (red) on the $d_{norm}$ surfaces. Other contacts (those weaker and longer contacts than the hydrogen bonds) are portrayed as diminutive spots and very light-colored areas. From Figures 6(a) and 6(b), both the hydrogen bond acceptors and donors are highlighted with large red spots on the Hirshfeld surfaces. It is clear that both the hydroxyl group and chlorine atom form strong intermolecular hydrogen bonds, the direction of these hydrogen bonds is also the direction of the strong interaction between venlafaxine hydrochloride molecules, and it also corresponds to the direction indicated by the blue and red lines in Figure 5(b). In Figure 6(c), the 2D-fingerprint plot of venlafaxine hydrochloride illustrates the nature and type of intermolecular contacts. Figure 6(d) gives the relative contributions of five types of intermolecular interactions. The H···H contacts between methyl and methylene groups of adjacent molecules are the most frequent interactions, which occupy 70.9% area. Meanwhile, O···H and Cl···H interactions make up 7.7% and 14.6% of the surface, respectively, revealing that hydrogen bonds are also dominant intermolecular interactions in venlafaxine hydrochloride crystal. In addition, there are small proportions of C···H (6.7%) and Cl···Cl (0.1%, halogen bonds) interactions in the crystal structure.

During the calculation of the vacuum morphology of venlafaxine hydrochloride, the AE ($E_{att}$) is also estimated besides the specific morphology; this allows us to quantitatively analyze the predicted crystal morphology. The higher the absolute value of the AE, the stronger the adsorption capacity of venlafaxine hydrochloride molecules on the crystal surface, which leads to the faster growth rate of the crystal face, and vice versa. As listed in Table II, the crystal faces at (1 1 0), (1 1 −1), (1 2 −1), (1 0 1), and (1 1 1) show the largest absolute value of AE over 140 kcal mol$^{-1}$, instead, the proportion of these faces in the total area is below 5%. On the other hand, the absolute values of the attachment energies of (0 2 0) and (0 1 1) are only 25.29 and 88.06 kcal mol$^{-1}$, but they account for 67.19% and 19.16% of the total areas, respectively. From the simulated shape shown in Figure 5(a), the area proportion of the crystal faces morphologically confirms the above results.

### C. Modified results of venlafaxine hydrochloride crystal morphology in solvent systems

MD simulation according to the MAE model was conducted in the solvent systems of isopropanol, dimethyl sulfoxide, and acetonitrile. Table III lists the simulation results of

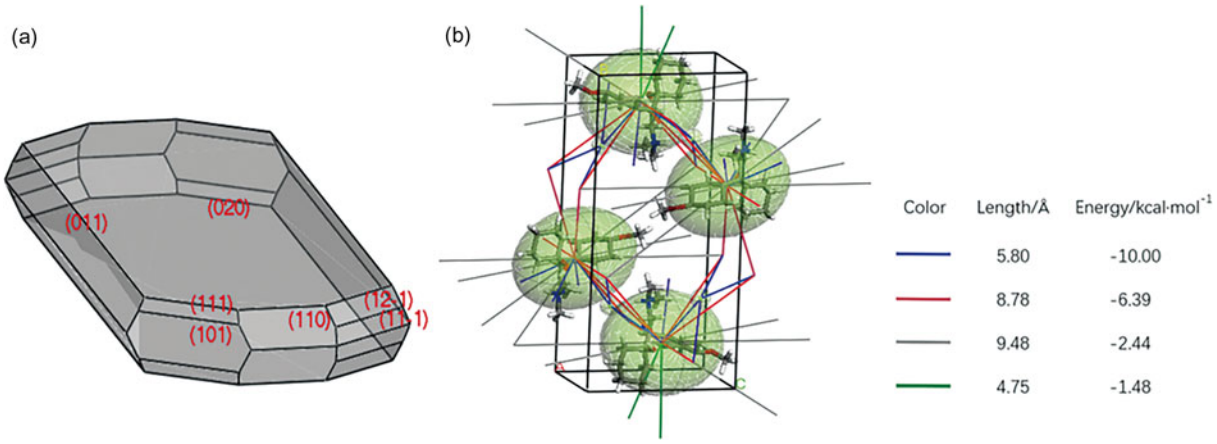


Figure 5. The predicted venlafaxine hydrochloride crystal morphology in the vacuum (a) and the intermolecular interactions in the venlafaxine hydrochloride unit cell calculated by the Crystal Graph (b).



https://doi.org/10.1017/S0885715622000264 Published online by Cambridge University Press

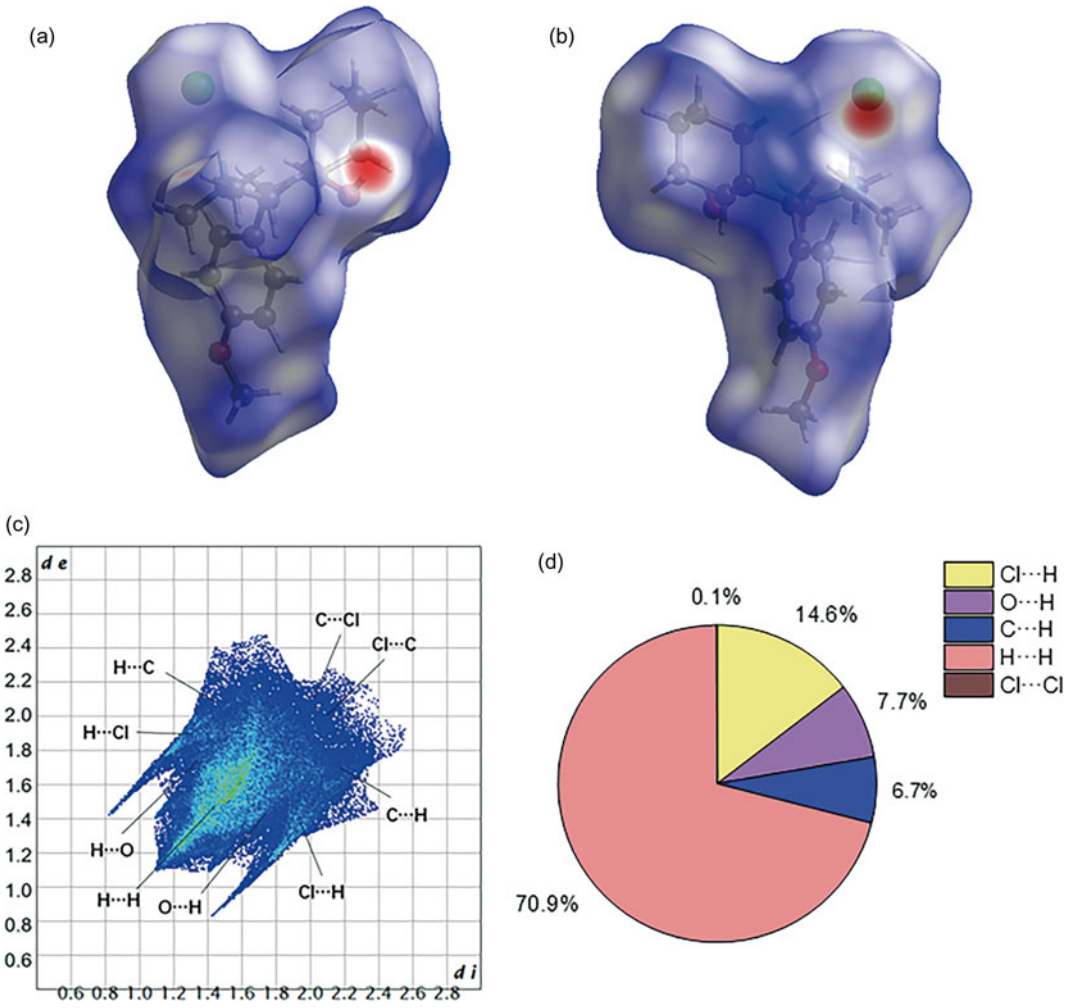


Figure 6. Hirshfeld surfaces (a) and (b), 2-D fingerprint plot (c), and relative contributions (d) to the Hirshfeld surface area for venlafaxine hydrochloride molecule in crystal.

seven significant crystal faces growing in the three solvents, respectively. Among them, the values of $E_{int}$ indicate the interaction energies between the solvents and the venlafaxine hydrochloride crystal faces. It is clear that no matter in which solvent, the final $E_{int}$ of the seven dominant crystal faces are negative, revealing it is a spontaneous process for absorbing the solvent molecule on the crystal faces. The diverse absolute values of $E_s$ for different crystal faces in the solvents can to some extent reflect the different solvent effects on each crystal face because of their distinct characteristics. Especially, the absolute values of $E_s$ of (0 2 0) faces are always the smallest, implying that the interactions between the solvents and crystal faces are relatively weak on the (0 2 0) faces. After correction according to the criteria, the absolute values of the MAE $|E'_{att}|$ are sorted as follows: (0 2 0) < (0 1 1) < (1 1 1) < (1 2 −1) < (1 1 −1) < (1 0 1) < (1 1 0) in isopropanol, (0 2 0) < (1 1 1) < (1 0 1) < (1 2 −1) < (0 1 1) < (1 1 −1) < (1 1 0) in dimethyl sulfoxide, and (0 0 2) < (1 1 1) < (1 0 1) < (0 1 1) < (1 2 −1) < (1 1 0) < (1 1 −1) in acetonitrile. Although the orders were not identical, the relatively most fastest-growing (1 1 0) face with the largest $|E'_{att}|$ disappears in all three solvent systems. Meanwhile, the (0 2 0) face occupies the largest percentage of the crystal facet areas of 42.18% in isopropanol, 62.79% in dimethyl sulfoxide, and 72.13% in acetonitrile, respectively, which is in good agreement with that of pole figures. Similarly, the proportions of other crystal faces change significantly compared to the calculation in vacuum because of their different growth rates according to their $|E'_{att}|$ value.

TABLE II. The parameters of the venlafaxine hydrochloride crystal faces in the vacuum predicted via the AE model.

| Faces ($h$ $k$ $l$) | Multiplicity | $d_{hkl}$ (Å) | $E_{att}$ (kcal mol$^{-1}$) | Area (%) |
|---|---|---|---|---|
| (0 2 0) | 2 | 13.03 | −25.29 | 67.19 |
| (0 1 1) | 4 | 10.59 | −88.06 | 19.16 |
| (1 1 0) | 4 | 5.65 | −157.69 | 4.33 |
| (1 1 −1) | 4 | 5.62 | −174.45 | 1.87 |
| (1 2 −1) | 4 | 5.26 | −165.82 | 2.18 |
| (1 0 1) | 2 | 4.75 | −141.72 | 3.52 |
| (1 1 1) | 4 | 4.67 | −142.32 | 1.74 |

As (1 1 0), (1 1 −1), (1 0 1), (0 1 1), or (1 2 −1) crystal faces disappear, the crystal morphology of venlafaxine hydrochloride obviously changed in the three solvent systems, which powerfully supported the non-negligible effects of the solvents on crystal habits. In Figure 7, the simulated crystals basically conform with the experimental ones with cubic hexagon, short rod, and long strip shape in isopropanol, dimethyl sulfoxide, and acetonitrile, respectively. The results explain the crystal forming mechanism from the



https://doi.org/10.1017/S0885715622000264 Published online by Cambridge University Press

TABLE III. Simulated results of the dominant crystal faces in isopropanol, dimethyl sulfoxide, and acetonitrile.

| Solvent | Faces | $E_{tot}$ | $E_{sol}$ | $E_{sur}$ | $E_{int}$ | $E_s$ | $E'_{att}$ | $R'_{hkl}$ | Area (%) |
|---|---|---|---|---|---|---|---|---|---|
| Isopropanol | (020) | −8381.73 | −5598.84 | −2672.21 | −110.68 | −14.61 | −10.68 | 1.00 | 42.18 |
| | (011) | −10 735.04 | −5327.58 | −4955.51 | −451.95 | −70.05 | −18.01 | 1.69 | 28.30 |
| | (110) | −10 256.46 | −5225.16 | −4402.36 | −628.94 | −94.34 | −63.35 | 5.93 | – |
| | (11-1) | −10 206.09 | −5226.36 | −4282.76 | −696.97 | −128.24 | −46.21 | 4.33 | – |
| | (12-1) | −10 257.42 | −5249.54 | −4168.83 | −839.05 | −140.96 | −24.86 | 3.08 | 16.08 |
| | (101) | −10 240.35 | −5232.10 | −4531.01 | −477.24 | −86.38 | −55.34 | 5.18 | – |
| | (111) | −10 040.59 | −5109.11 | −4104.00 | −827.48 | −165.50 | 23.17 | 2.17 | 13.44 |
| Dimethyl sulfoxide | (020) | −2979.99 | −68.18 | −2692.80 | −219.01 | −28.91 | 3.62 | 1.00 | 62.79 |
| | (011) | −5227.82 | 62.75 | −4962.57 | −328.00 | −50.84 | −37.22 | 10.28 | – |
| | (110) | −4893.70 | 288.77 | −4426.43 | −756.04 | −113.40 | −44.29 | 12.23 | – |
| | (11-1) | −4686.60 | 282.97 | −4258.77 | −710.79 | −130.79 | −43.67 | 12.06 | – |
| | (12-1) | −4634.12 | 394.07 | −4185.49 | −842.70 | −141.57 | −24.25 | 6.70 | 10.33 |
| | (101) | −4830.95 | 420.78 | −4525.23 | −726.50 | −131.50 | −10.23 | 2.83 | – |
| | (111) | −4459.72 | 346.72 | −4048.00 | −758.44 | −151.69 | 9.37 | 2.59 | 26.88 |
| Acetonitrile | (020) | −4318.06 | −1491.52 | −2646.31 | −180.23 | −23.79 | −1.5 | 1.00 | 72.13 |
| | (011) | −6580.62 | −1275.68 | −4962.94 | −342.00 | −53.01 | −35.05 | 23.37 | 3.24 |
| | (110) | −6230.54 | −1143.96 | −4375.24 | −711.34 | −106.70 | −50.99 | 34.00 | – |
| | (11-1) | −6076.24 | −1133.06 | −4292.59 | −650.59 | −119.71 | −54.74 | 36.49 | – |
| | (12-1) | −6047.66 | −1131.12 | −4231.78 | −684.76 | −115.04 | −50.78 | 25.85 | – |
| | (101) | −6261.11 | −1019.59 | −4353.10 | −888.42 | −160.80 | 19.08 | 12.72 | – |
| | (111) | −5918.91 | −1004.88 | −4178.91 | −735.12 | −147.02 | 4.70 | 3.13 | 24.63 |

All energies are in kcal $mol^{-1}$.

thermodynamic point of view and further verify the reliability of the crystal face growth by simulation prediction. In addition, more detailed and microscopic research will help us to have a deeper understanding of the interaction between crystals and solvents, better directional control of crystal shapes, and faster and more economical selection of solvents suitable for industrial crystallization.

### D. Solvent–crystal interactions on the interface

As discussed above, the MAE indicates that there is an interaction between the solvent layer and the crystal layer in the box, an interaction which has a decisive influence on the final morphology of the crystal. In practice, one can thoroughly understand the influence of solvent on crystal morphology by combining the interface contact properties and the non-bonding of crystal–solvent molecules. In this study, the anisotropy of venlafaxine hydrochloride crystal structure leads to a distinct molecular alignment on each crystal face and then gives rise to a different solvent molecular distribution at the solvent–crystal interface. The difference caused by different molecular surface structures has a crucial influence on the adsorption of solvents on crystal face and finally leads to the change in crystal growth and morphology.

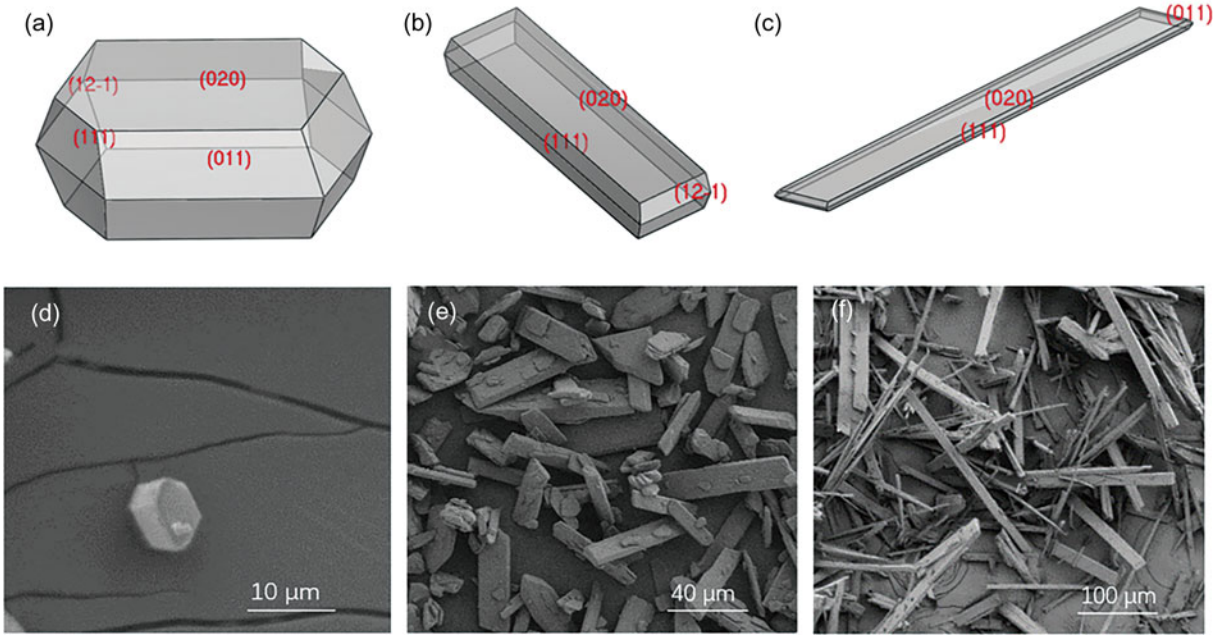


Figure 7. The predicted crystal morphology of venlafaxine hydrochloride in (a) isopropanol, (b) dimethyl sulfoxide, and (c) acetonitrile via the MAE model and the corresponding SEM images of the experimental products in (d) isopropanol, (e) dimethyl sulfoxide, and (f) acetonitrile.



https://doi.org/10.1017/S0885715622000264 Published online by Cambridge University Press

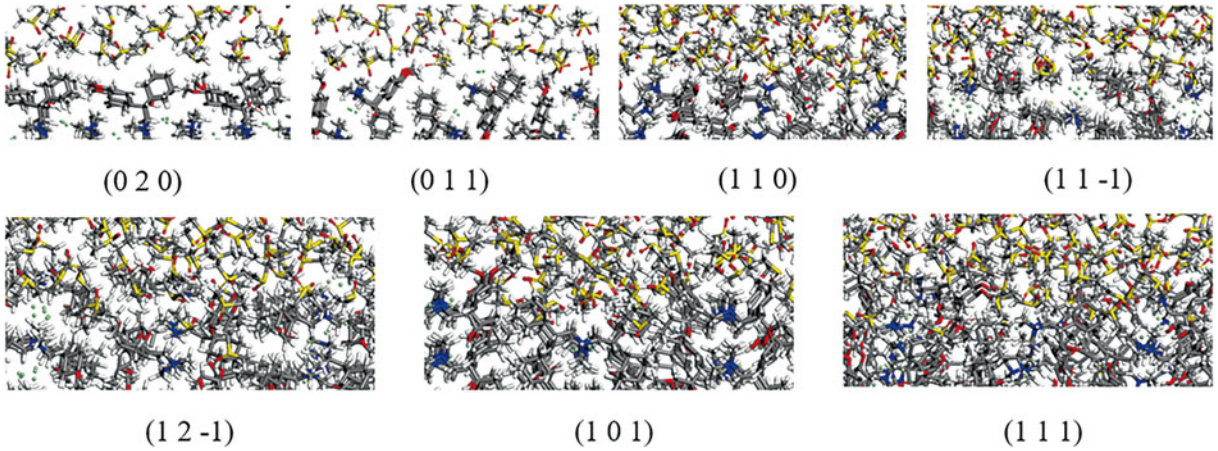


Figure 8. Adsorption equilibrium structures of crystal face and dimethyl sulfoxide after MD calculation.

TABLE IV. The roughness values ($S$) of the dominant crystal faces of the venlafaxine hydrochloride crystal.

| Faces ($h$ $k$ $l$) | $A_{hkl}$ (Å$^2$) | $A_{acc}$ (Å$^2$) | $S$ |
|---|---|---|---|
| (0 2 0) | 71.085 | 84.565 | 1.190 |
| (0 1 1) | 170.763 | 238.500 | 1.397 |
| (1 1 0) | 319.040 | 431.605 | 1.353 |
| (1 1 −1) | 320.885 | 531.615 | 1.657 |
| (1 2 −1) | 343.953 | 521.590 | 1.516 |
| (1 0 1) | 379.231 | 618.735 | 1.632 |
| (1 1 1) | 389.009 | 701.490 | 1.803 |

### 1. Surface structure

In the process of crystal growth, solvent molecules constantly contact solute molecules through diffusion, and a large number of solvent molecules are adsorbed on the crystal surface layer, finally forming a stable structure. In order to explain how the surface structure affected the interaction between crystal and solvent, MD-simulated equilibrium configurations of the interface model for venlafaxine hydrochloride and dimethyl sulfoxide molecules were typically calculated as an example.

From Figure 8, one can clearly see that owing to the different surface structures of each crystal face, the contact mode between dimethyl sulfoxide molecules and seven crystal faces is not exactly the same. Compared with the other six faces, venlafaxine hydrochloride molecules on crystal faces (0 2 0) are relatively parallel to the crystal faces, so the periodic crystal faces formed in the direction are relatively smooth, which can provide fewer contact sites for solutes and solvents. However, venlafaxine hydrochloride molecules on the remaining six surfaces all form a certain angle with the crystal faces, leading to a bumpy surface. More grooves mean more adsorption sites and stronger adsorption capacity for solute and solvent molecules. Therefore, the contact between the solvent molecules on these six faces is closer than that of crystal faces (0 2 0).

Whether the contact between the solvent layer and the crystal face is dense or not will affect the growth rate of the crystal face to a certain extent, which may be one of the reasons why the (0 2 0) faces account for a large proportion in all crystals obtained from the three solvents. In addition, the molecular alignment makes polar hydroxyl groups and chlorine atoms exposed on crystal surfaces, which is more favorable to the adsorption of solvent molecules on the crystal surface. Different positions and angles of the exposed groups may form various non-bonding interactions and provide different adsorption areas for solvent molecules.

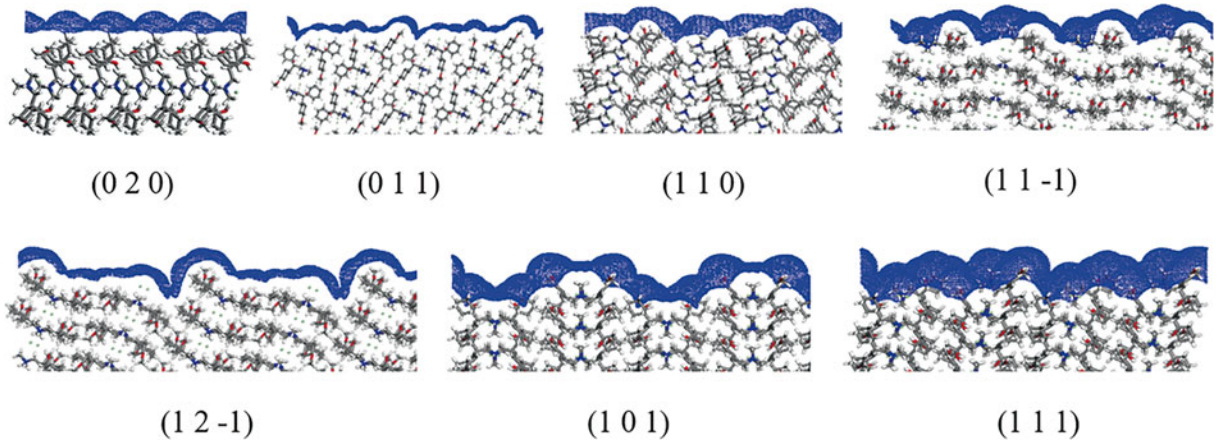


Figure 9. Solvent-accessible areas (the blue grid) of the seven dominant faces of the venlafaxine hydrochloride crystal represented by the Connolly surface.



https://doi.org/10.1017/S0885715622000264 Published online by Cambridge University Press

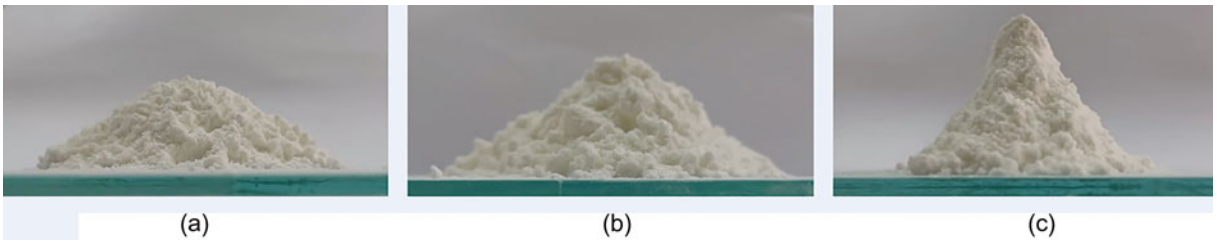


Figure 10. The conical piles graphs of the venlafaxine hydrochloride recrystallization from (a) isopropanol, (b) dimethyl sulfoxide, and (c) acetonitrile, respectively.

### 2. Roughness of surfaces

To quantitatively analyze the structural features of crystal face, a parameter $S$ is usually introduced to evaluate the roughness of crystal surfaces according to Zhao *et al.* (2016), which can be expressed by the below formula.

$$S = A_{\mathrm{acc}}/A_{hkl}$$

Here, $A_{\mathrm{acc}}$ and $A_{hkl}$ represent the solvent-accessible area and surface area for the ($h$ $k$ $l$) crystal surface in the unit cell, respectively. The value of $S$ is proportional to the surface roughness, that is, the larger $S$ is, the rougher the crystal surface is, implying a more complex surface. Thus, a larger $S$ may result in the larger energy correction term, $Es$, and dramatically influence the final morphology. Table IV lists the calculated $S$ values of the crystal faces.

To understand the surface structure of crystal face and the interactions of solvent molecules with different venlafaxine hydrochloride crystal surfaces more intuitively, the molecular packing structures of venlafaxine hydrochloride are displayed in Figure 9 with a Connolly surface model. The blue grids on the venlafaxine hydrochloride crystal surface show the accessible solvent surface. It is clear that although the shape of the solvent-accessible area of each crystal face is different, the solvent-accessible area fluctuates periodically with the cycle of the unit cell, following form more grooves with a larger contact area between crystal surfaces and solvent molecules.

As listed in Table IV, the order of the roughness values for the seven crystal faces is (0 2 0) < (0 1 1) < (1 1 −1) < (1 1 0) < (1 2 −1) < (1 0 1) < (1 1 1). The (0 2 0) face with the smallest $S$ value (1.23) provides the minimum areas for molecule incorporation, which means it was probably difficult for solvent and solute molecules to adsorb on this face compared with the other faces. This is consistent with the relatively slow growth rate of the (0 2 0) face, resulting in a largest face area as shown in Figure 7. On the contrary, the (1 1 1) faces with the larger $S$ value remain a smaller face area after growth.

TABLE V. Compressibility performance data of venlafaxine hydrochloride powders prepared from three solvents.

| Solvent | AoR (°) | Bulk density (g cm$^{-3}$) | Tap density (g cm$^{-3}$) | Compressibility % |
|---|---|---|---|---|
| IPA | 31.9 ± 0.1 | 0.512 | 0.597 | 16.6 |
| DMSO | 36.5 ± 0.1 | 0.405 | 0.501 | 19.8 |
| ACN | 55.7 ± 0.1 | 0.325 | 0.473 | 45.5 |

## V. POWDER PROPERTIES ANALYSIS

Investigation of the flowability of the drug is an important part of its physical and chemical characterization, which was performed under a specified set of conditions (Zatloukal and Šklubalová, 2008; Xu *et al.*, 2018). Measurement of Angle of Repose (AoR) is acknowledged as one of the methods for quickly determining the nature of powder flowability. In the study, the static AoR measurement was adopted by pouring the powder through a funnel-defined geometry. The obtained conical piles are shown in Figure 10.

After five measurements, the average values of the AoR were calculated and listed in Table V. Generally, it is considered that the smaller the angle of repose, the better its flowability. From Table V, the AoRs of crystals formed in isopropanol, dimethyl sulfoxide, and acetonitrile are about 31.9°, 36.5°, and 55.7°, respectively, exhibiting significant differences accompanying the morphology change. It is clear that the crystals obtained from isopropanol have best flowability; on the contrary, the worst in acetonitrile.

In addition, the compressibility performance of the crystal products was also analyzed and the results were shown in Table V. It is generally acknowledged that when the compressibility is less than 20%, the flowability of powder is good. According to the data in Table V, the crystals obtained from isopropanol have a best compressibility of 16.6%, but it is 45.5% for the crystals obtained from acetonitrile, the conclusion from this aspect is consistent with the conclusion of the angle of repose.

The testing results further confirm that the morphology of the drug crystals determines its physical properties, suggesting it is feasible to screen the most suitable drug crystals through crystal growth model building.

## VI. CONCLUSIONS

In this paper, the crystal morphologies of venlafaxine hydrochloride in three solvents of acetonitrile, dimethyl sulfoxide, and isopropanol were successfully predicted by the MAE model which takes solvent effects into consideration. The results suggest that the simulated crystal habits are in good agreement with the experimental results of recrystallization. To explain it from the molecular point of view, the solvent–crystal adsorption interface models are further built to study the adsorption interactions between venlafaxine hydrochloride crystal surfaces and solvent molecules.

For venlafaxine hydrochloride crystals, the (0 2 0) face is the most morphologically dominant crystal face because of its small MAE and relatively flat surface, leading to a relatively



https://doi.org/10.1017/S0885715622000264 Published online by Cambridge University Press

slow face growth. The molecular alignment and roughness analysis on dominant crystal faces indicate that the (1 1 0) face disappeared in final crystal morphology because of the competitive adsorption of molecules favorable for solutes to continuously adsorb on the surface. Owing to the difference of the MAE and physical characteristics of each crystal face, the growth of venlafaxine hydrochloride crystals shows significant anisotropy in different solvents, resulting in various crystal morphology, which further affects the angle of repose and compressibility of drug powder.

## ACKNOWLEDGEMENTS

The work was supported by the National Natural Science Foundation of China (Grants No. 22075252).

## CONFLICTS OF INTERESTS

The authors declare no conflicts of interest.

Andrews, J. M., Ninan, P. T., and Nemeroff, C. B. (**1996**). "Venlafaxine: a novel antidepressant that has a DUAL mechanism of action," J. Depression **4**, 48–56.

Chen, F., Zhou, T., and Wang, M. (**2020**). "Spheroidal crystal morphology of RDX in mixed solvent systems predicted by molecular dynamics," J. Phys. Chem. Solids **136**, 109196.

Dzade, N. Y., Roldan, A., and de Leeuw, N. H. (**2016**). "Surface and shape modification of mackinawite (FeS) nanocrystals by cysteine adsorption: a first-principles DFT-D2 study," Phys. Chem. Chem. Phys. **18**, 32007–32020.

Graaf, J., Filion, L., Marechal, M., Roij, R., and Dijkstra, M. (**2012**). "Crystal-structure prediction via the floppy-box Monte Carlo algorithm: method and application to hard (non)convex particles," Chem. Phys. **137**, 214101.

Hartman, P. and Bennema, P. (**1980**). "The attachment energy as a habit controlling factor I. Theoretical considerations," J. Cryst. Growth **49**, 145–156.

Jiang, Y., Xu, J., and Zhang, H. (**2013**). "Research progress on HMX crystallization morphology," J. Mater. Renew. **27**, 11–17.

Khoshkhoo, S. and Anwar, J. (**1996**). "Study of the effect of solvent on the morphology of crystals using molecular simulation: application to $\alpha$-resorcinol and N-n-octyl-D-gluconamide," J. Chem. Soc. Faraday Trans. **92**, 1023–1025.

Kitamura, M. and Ishizu, T. (**2000**). "Growth kinetics and morphological change of polymorphs of L-glutamic acid," J. Cryst. Growth **209**, 138–145.

Lecrubier, Y., Bourin, M., Moon, C. A. L., Schifano, F., Blanchard, C., Danjou, P., and Hackett, D. (**1997**). "Efficacy of venlafaxine in depressive illness in general practice," Acta Psychiatr. Scand. **95**, 485–493.

Li, J., Jin, S., Lan, G., Xu, Z., Wu, N., Chen, S., and Li, L. (**2019**). "The effect of solution conditions on the crystal morphology of $\beta$-HMX by molecular dynamics simulations," J. Cryst. Growth **507**, 38–45.

Liu, Y. (**2021**). "Crystal morphology prediction method of energetic materials: attachment energy model and Its development," J. Chinese J. Explosives & Propellants **44**, 578–588.

Liu, J., Chang, Z., He, Y., Yang, M., and Dang, J. (**2007**). "Solvent effects on the crystallization of avermectin B1a," J. Cryst. Growth **307**, 131–136.

MacLeod, C. S., and Muller, F. L. (**2012**). "On the fracture of pharmaceutical needle-shaped crystals during pressure filtration: case studies and mechanistic understanding," J. Org. Process Res. Dev. **16**, 425–434.

Mckinnon, J. J., Jayatilaka, D., and Spackman, M. A. (**2007**). "Towards quantitative analysis of intermolecular interactions with Hirshfeld surfaces," J. Chem. Commun. **37**, 3814–3816.

Miroslav, V., Peter, S., Jan, L., and Eva, V. (**2012**). "Crystal habit modifications of imatinib mesylate under various precipitation conditions," J. Monatsh Chem. **143**, 65–71.

Olver, J. S., Burrows, G. D., and Norman, T. R. (**2001**). "Third-generation antidepressants," J. CNS Drugs **15**, 941–954.

Parmar, M. M., Khan, O., Seton, L., and Ford, J. L. (**2007**). "Polymorph selection with morphology control using solvents," J. Cryst. Growth Des. **7**, 1635–1642.

Salvalaglio, M., Vetter, T., Giberti, F., Mazzotti, M., and Parrinello, M. (**2012**). "Uncovering molecular details of urea crystal growth in the presence of additives," J. Am. Chem. Soc. **134**, 17221–17233.

Sivalakshmidevi, A., Vyas, K., Mahender, R., and Reddyb, G. (**2002**). "A monoclinic polymorph of venlafaxine hydrochloride," J. Acta Cryst. **58**, 1072–1074.

Spackman, M. A., and Jayatilaka, D. (**2009**). "Hirshfeld surface analysis," J. Cryst. Eng. Comm. **11**, 19–32.

Spackman, M. A., and Mckinnon, J. J. (**2002**). "Fingerprinting intermolecular interactions in molecular crystals," J. Cryst. Eng. Comm. **4**, 378–392.

Ter Horst, J. H., Kramer, H. J. M., Rosmalen, G. M., and Jansens, P. J. (**2002**). "Molecular modelling of the crystallization of polymorphs. Part I: the morphology of HMX polymorphs," J. Cryst. Growth **237**, 2215–2220.

Urbelis, J. H., and Swift, J. A. (**2014**). "Solvent effects on the growth morphology and phase purity of CL-20," J. Cryst. Growth Des. **14**, 1642–1649.

Weissbuch, I., Addadi, L., Lahav, M., and Leiserowitz, L. (**1991**). "Molecular recognition at crystal interfaces," J. Sci. **253**, 637–645.

Xu, T., and Wang, Y. (**2017**). "Quantitative determination of venlafaxine hydrochloride polymorphs using X-ray powder diffractometry," Chinese J. New Drugs **26**, 2614–2619.

Xu, G., Lu, P., Li, M., Liang, C., Xu, P., Liu, D., and Chen, X. (**2018**). "Investigation on characterization of powder flowability using different testing methods," Exp. Therm. Fluid Sci. **92**, 390–401.

Zatloukal, Z., and Šklubalová, Z. (**2008**). "Drained angle of free-flowable powders," Part. Sci. Technol. **26**, 595–607.

Zhang, W., Chen, C., and Zhang, S. (**2013**). "Equilibrium crystal shape of Ni from first principles," J. Phys. Chem. C **117**, 21274–21280.

Zhang, M., Liang, Z., Wu, F., and Chen, J. (**2017**). "Crystal engineering of ibuprofen compounds: from molecule to crystal structure to morphology prediction by computational simulation and experimental study," J. Cryst. Growth **467**, 47–53.

Zhao, Q., Liu, N., Wang, B., and Wang, W. (**2016**). "A study of solvent selectivity on the crystal morphology of FOX-7 via a modified attachment energy model," J. RSC Adv. **6**, 59784–59793.

Zhu, D., Zhang, S., Cui, P., Wang, C., Dai, J., Zhou, L., *et al*. (**2020**). "Solvent effects on catechol crystal habits and aspect ratios: a combination of experiments and molecular dynamics simulation study," J. Crystals **10**, 316–332.